4. F. Grein, A. R. Ramos, S. S. Venceslau, I. A. C. Pereira, *Biochim. Biophys. Acta* **1827**, 145–160 (2013).
5. A. L. Müller, K. U. Kjeldsen, T. Rattei, M. Pester, A. Loy, *ISME J.* **9**, 1152–1165 (2015).
6. H. D. Peck Jr., J. LeGall, J. VanBeeumen, *Philos. Trans. R. Soc. Lond., B* **298**, 443–466 (1982).
7. A. S. Bradley, W. D. Leavitt, D. T. Johnston, *Geobiology* **9**, 446–457 (2011).
8. B. Brunner, S. M. Bernasconi, *Geochim. Cosmochim. Acta* **69**, 4759–4771 (2005).
9. W. D. Leavitt, A. S. Bradley, A. A. Santos, I. C. Pereira, D. T. Johnson, *Front. Microbiol.* **6**, 1392 (2015).
10. T. F. Oliveira *et al.*, *J. Biol. Chem.* **283**, 34141–34149 (2008).
11. S. S. Venceslau, Y. Stockdreher, C. Dahl, I. A. C. Pereira, *Biochim. Biophys. Acta* **1837**, 1148–1164 (2014).
12. K. L. Keller *et al.*, *Appl. Environ. Microbiol.* **80**, 855–868 (2014).
13. D. E. Canfield *et al.*, *Science* **330**, 1375–1378 (2010).
14. F. J. Stewart, O. Dmytrenko, E. F. Delong, C. M. Cavanaugh, *Front. Microbiol.* **2**, 134 (2011).
15. Y. Ikeuchi, N. Shigi, J. Kato, A. Nishimura, T. Suzuki, *Mol. Cell* **21**, 97–108 (2006).
16. K. Parey, E. Warkentin, P. M. H. Kroneck, U. Ermler, *Biochemistry* **49**, 8912–8921 (2010).
17. K. Parey, G. Fritz, U. Ermler, P. M. H. Kroneck, *Metallomics* **5**, 302–317 (2013).
18. Materials and methods are available as supplementary materials on *Science* Online
19. Y. C. Hsieh *et al.*, *Mol. Microbiol.* **78**, 1101–1116 (2010).
20. M. Wagner, A. J. Roger, J. L. Flax, G. A. Brusseau, D. A. Stahl, *J. Bacteriol.* **180**, 2975–2982 (1998).
21. T. Ida *et al.*, *Proc. Natl. Acad. Sci. U.S.A.* **111**, 7606–7611 (2014).
22. B. D. Paul, S. H. Snyder, *Nat. Rev. Mol. Cell Biol.* **13**, 499–507 (2012).
23. Y. Liu *et al.*, *J. Biol. Chem.* **287**, 36683–36692 (2012).
24. R. W. Nielsen, C. Tachibana, N. E. Hansen, J. R. Winther, *Antioxid. Redox Signal.* **15**, 67–75 (2011).
25. R. H. Pires *et al.*, *Biochemistry* **45**, 249–262 (2006).
26. R. Hedderich, N. Hamann, M. Bennati, *Biol. Chem.* **386**, 961–970 (2005).
27. F. Grein, I. A. C. Pereira, C. Dahl, *J. Bacteriol.* **192**, 6369–6377 (2010).

ACKNOWLEDGMENTS

We thank R. Soares for the mass spectrometry measurements, C. Leitão for HPLC technical support, and H. Santos and L. Gafeira for providing *A. fulgidus*. We also thank J. Wall for plasmids for genetic manipulation of *D. vulgaris*, A. Ramos for technical assistance, A. Masterson for synthesis of the trithionate standard, A. Bradley for detailed discussions, and W. Martin for critical reading of the manuscript. This work was funded by grants from NSF-EAR (1225980 to D.T.J. and I.A.C.P.), from Fundação para a Ciência e a Tecnologia (FCT), Portugal (UID/Multi/04551/2013, PTDC/QUI-BIQ/100591/2008, and PTDC/BBB-BQB/0684/2012) and Deutsche Forschungsgemeinschaft, Germany (Da 351/6-2). A.S. and S.S.V. are recipients of FCT fellowships (SFRH/BD/77940/2011 and SFRH/BPD/79823/2011). W.D.L. acknowledges support by an NSF–Graduate Research Fellowship Program and the Fossett Fellowship from Washington University in St. Louis. The data reported in this paper are provided in the supplementary materials.

SUPPLEMENTARY MATERIALS

www.sciencemag.org/content/350/6267/1541/suppl/DC1
Materials and Methods
Figs. S1 to S15
Tables S1 to S3
References (*28*–*41*)

2 September 2015; accepted 4 November 2015
10.1126/science.aad3558

ECOTOXICOLOGY

Algal toxin impairs sea lion memory and hippocampal connectivity, with implications for strandings

Peter F. Cook,[1,2]* Colleen Reichmuth,[2] Andrew A. Rouse,[2] Laura A. Libby,[3] Sophie E. Dennison,[4] Owen T. Carmichael,[5] Kris T. Kruse-Elliott,[4] Josh Bloom,[4] Baljeet Singh,[3] Vanessa A. Fravel,[6] Lorraine Barbosa,[6] Jim J. Stuppino,[4] William G. Van Bonn,[7] Frances M. D. Gulland,[6] Charan Ranganath[3]

Domoic acid (DA) is a naturally occurring neurotoxin known to harm marine animals. DA-producing algal blooms are increasing in size and frequency. Although chronic exposure is known to produce brain lesions, the influence of DA toxicosis on behavior in wild animals is unknown. We showed, in a large sample of wild sea lions, that spatial memory deficits are predicted by the extent of right dorsal hippocampal lesions related to natural exposure to DA and that exposure also disrupts hippocampal-thalamic brain networks. Because sea lions are dynamic foragers that rely on flexible navigation, impaired spatial memory may affect survival in the wild.

Domoic acid (DA) is an amino acid neurotoxin that causes neurological symptoms in marine animals, most visibly California sea lions (CSLs, *Zalophus californianus*) (*1*). As a result of environmental change and human impacts on marine systems, the size and frequency of DA-producing *Pseudonitszchia* algal blooms are increasing (*2*), and toxic exposure is widespread in CSLs (*3*). Although exposed CSLs show a reliable and specific pattern of seizures and hippocampal lesions (*4*), the sublethal effects on behavior are unclear. In rodents and humans, the hippocampus is necessary for spatial memory (*5*, *6*). As dynamic central-place foragers (*7*), CSLs may be especially vulnerable to spatial memory deficits, and anecdotal data from postrehabilitation tracking show unusual movement patterns in exposed animals (*8*). Together, these observations suggest that DA exposure in CSLs and resultant hippocampal damage could be associated with impaired spatial memory. In this study, we used controlled behavioral studies, integrated with prerelease veterinary care and structural and functional neuroimaging, to directly test this hypothesis in wild sea lions.

Between April 2009 and November 2011, we studied 30 wild CSLs undergoing veterinary care and rehabilitation (table S1). Drawing from the literature on hippocampal function in rodents, we developed two spatial memory assays and compared performances with hippocampal volumes, measured using in vivo magnetic resonance imaging (MRI). The hippocampus was manually traced (fig. S1), and structural volumes were calculated as percentages of total brain volume for each animal (*9*). Veterinary diagnosis predicted hippocampal volume [repeated measures analysis of variance (ANOVA): $F = 16.25$, df = 1, $P < 0.001$] (*9*), justifying the use of volume as the primary independent variable. Given the magnitude and range of hippocampal volumes across the sample, subsequent analyses treated volume as a continuous variable.

Because lesions are typically unilateral in this population (*3*), and because other species show lateralization of hippocampal function (*10*), right and left hippocampal volumes were regressed separately with behavioral performance. In some species, spatial memory is more reliant on the septal (dorsal) than on the temporal (ventral) hippocampus (*11*). Accordingly, we divided the hippocampi in half by length and conducted follow-up regression analyses with ventral and dorsal hippocampal volumes (*9*). We report these results when they differ from those expected based on analyses of the entire longitudinal extent of the hippocampus. Rodent data suggest that the dorsal third of the hippocampus may be sufficient to support spatial memory (*11*), so in cases where the dorsal half was a significant predictor of behavior, we conducted follow-up analyses that

[1]Center for Neuropolicy, Emory University, Atlanta, GA 30322, USA. [2]Pinniped Cognition and Sensory Systems Laboratory, Institute of Marine Sciences, University of California–Santa Cruz, Santa Cruz, CA 95060, USA. [3]Dynamic Memory Lab, Center for Neuroscience, University of California–Davis, Davis, CA 95618, USA. [4]AnimalScan Advanced Veterinary Imaging, Redwood City, CA 94063, USA. [5]Pennington Biomedical Research Center, Baton Rouge, LA 70808, USA. [6]The Marine Mammal Center, Sausalito, CA 94965, USA. [7]Shedd Aquarium, Chicago, IL 60605, USA.
*Corresponding author. E-mail: pfcook@emory.edu

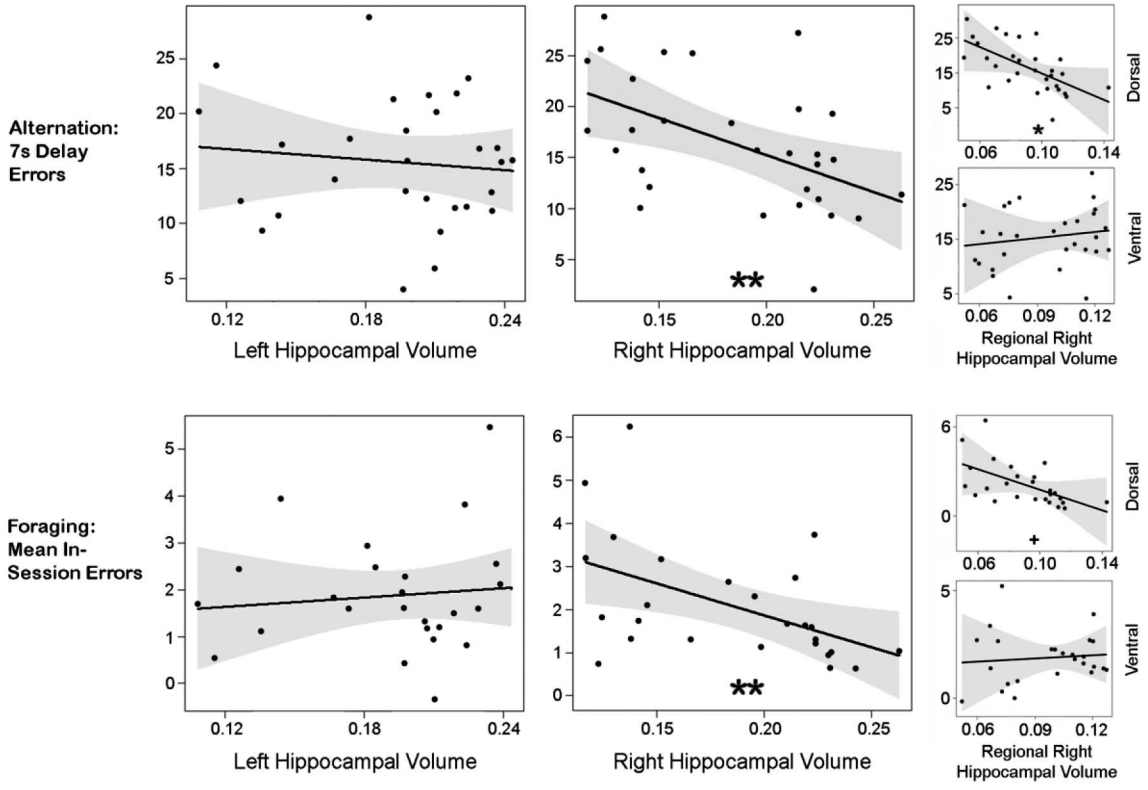

Fig. 1. Spatial memory is related to the integrity of the right hippocampus. The conditional scatterplots show correlations between left and right hippocampal volumes (as a percentage of total brain volume; *x* axes) and performance measures (*y* axes) related to behavioral alternation and foraging tasks, after regressing out other dependent variables. Regression analyses for alternation included no-delay test errors as an independent variable to control for variance in test performance that was unrelated to memory. Alternation, right: $t = -2.82$, df = 27, $P < 0.01$. Alternation, left: $t(0.54) < 1$, df = 27. Foraging, right: $t = -2.66$, df = 23, $P < 0.01$. Foraging, left: $t(0.5) < 1$, df = 23. The insets on the right show correlations of ventral and dorsal right hippocampal volumes with performance measures after regressing out other dependent variables. Alternation, dorsal: $t = -2.05$, df = 27, $P < 0.05$. Alternation, ventral: $t(0.235) < 1$, df = 27. Foraging, dorsal: $t = -1.72$, df = 23, $P < 0.1$. Foraging, ventral: $t(0.33) < 1$, df = 23. Confidence bands for fit lines are shown in gray. Each point represents one animal. $^{+}P < 0.1$; $^{*}P < 0.05$; $^{**}P < 0.01$.

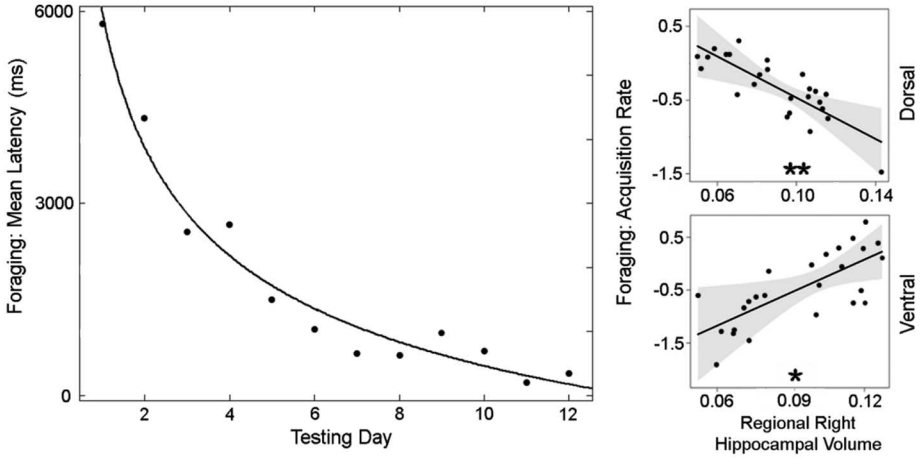

Fig. 2. Dissociable contributions of the dorsal and ventral right hippocampus to long-term spatial memory. Mean latency (to finding a reward) across all subjects is shown as a function of testing day [curve: $y = a*x^b + c$, coefficient of determination (R^2) = 0.97]. The inset conditional plots (right) show correlations between dorsal and ventral right hippocampal volume (as a percentage of total brain volume; *x* axes) and the foraging acquisition rate [log-transformed latency per testing day, *y* axes; represented as the slope of the logged power curve, with the steeper negative slope (faster acquisition) lower on the axis] after regressing out other dependent variables. Dorsal: $t = -3.21$, df = 21, $P < 0.005$. Ventral: $t = 2.44$, df = 21, $P < 0.05$. $^{*}P < 0.05$; $^{**}P < 0.01$.

substituted the volume of the dorsal third. Results were comparable to the dorsal half analyses (*9*).

The first behavioral task involved spatial alternation in a two-choice maze (fig. S2). Delayed alternation performance is impaired by hippocampal lesions in rodents (*12*) and is believed to rely on the role of the hippocampus in representing and sequencing memory for recent navigational episodes (*6*). After training to a baseline success rate of 85% on free-running left-right alternation (movie S1) (*9*), each sea lion was presented with 40 delay trials, in which the animals had to wait for 7 s at the beginning of each trial before entering the maze (movie S2). Delay trials were paired with 40 no-delay comparison trials. Right, but not left, hippocampal volume positively correlated with performance on delay trials. In addition, dorsal, but not ventral, right hippocampal volume positively correlated with performance (Fig. 1).

The second behavioral assessment was a spatial foraging task in which four possible food locations (opaque buckets) were made available once every 24 hours in the animals' enclosure (fig. S3 and movie S3). For each animal, one set location always contained food, while the others did not. At the beginning of a test session, subjects received fish at a central location while the buckets were simultaneously presented. Latency to the correct location across sessions and mean within-session errors (revisits to previously visited locations) were recorded (*9*). Rodent data indicate that within-session errors in similar spatial choice tasks track hippocampal damage (*13*). In our subjects,

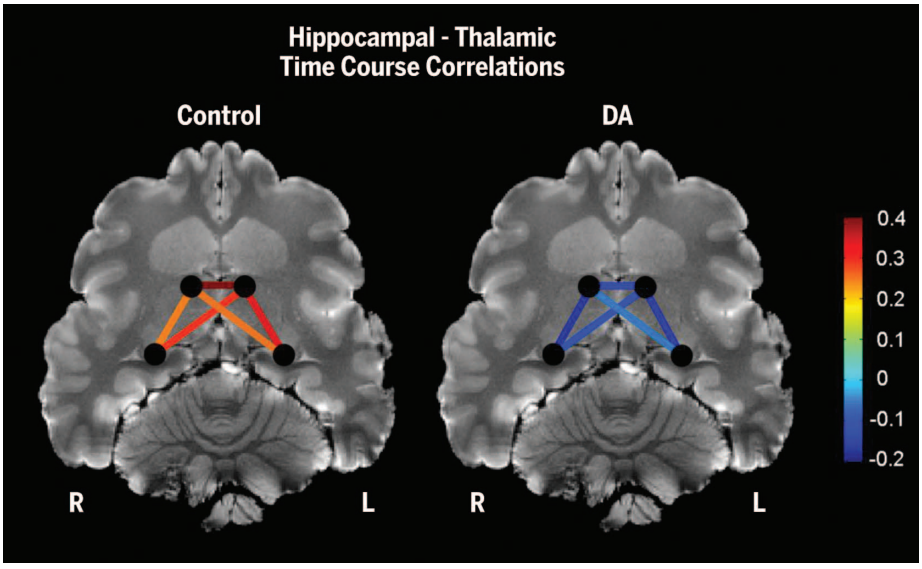

Fig. 3. Altered hippocampal-thalamic connectivity in animals with hippocampal lesions. Shown are maps of hippocampal-thalamic correlation coefficients, averaged for five brains with hippocampal lesions (right) and six without (left). The colors of the lines connecting regions of the brain represent the correlation strength of their respective time courses, with warmer colors indicating higher correlations.

right, but not left, hippocampal volume was positively correlated with within-session performance (Fig. 1).

To assess longer-term spatial memory, an additional performance measure was extracted from the foraging task. Because the mean cross-session learning curve for all animals was fit nearly perfectly by a power function (Fig. 2), the slope of the logged power curve for each animal was used to index the cross-session learning rate (table S3). Neither right nor left hippocampal damage was predictive of learning rate across all sessions (table S4). However, individual learning rates correlated positively with dorsal right hippocampal volumes and negatively with ventral right hippocampal volumes (Fig. 2).

The data reviewed thus far suggest a direct relationship between right hippocampal structure and spatial memory in sea lions. Spatial memory also depends on dynamic interactions between the hippocampus and other brain regions (*14*), with the hippocampal-thalamic axis being particularly relevant (*15*). CSLs with DA toxicosis present with seizures (*3*), which alter hippocampal networks in rodents (*16*). Accordingly, we used functional MRI to examine hippocampal-thalamic functional connectivity (*17*) in 11 CSLs undergoing rehabilitation between August and October 2012 (table S2). Five of the 11 showed volumetric evidence of gross hippocampal lesions (*9*). The other six animals served as a provisional control group. Although their complete ecotoxicant exposure history was not available, independent assessment by a veterinary radiologist and veterinarian found no evidence of neurological abnormality (*9*).

Animals with hippocampal lesions showed reduced hippocampal-thalamic connectivity (repeated measures ANOVA: $F = 22.3$, df = 1, $P < 0.001$) (Fig. 3). Reductions in connectivity were bilateral, with no statistical interaction between group (DA versus control) and laterality [$F(0.003) < 1$, df = 1] (*9*). A subsequent voxel-wise test showed high hippocampal-thalamic connectivity in controls (fig. S5) (*9*).

These data combining behavioral and neural measures in wild sea lions suggest that spatial memory is impaired and hippocampal-thalamic connectivity is disrupted as a result of DA-related hippocampal damage. The functional lateralization matches that found in humans (*10*) and may be consistent with findings of functional cortical asymmetry in sea lions (*18*). Because we examined wild CSLs, the effects of non–DA-related neurological insults were not fully controlled. This limitation is also a strength, because our results directly generalize to wild individuals.

Impairment in short- and long-term spatial memory as a result of hippocampal lesions and altered hippocampal networks probably interferes with foraging in CSLs and could partly explain maladaptive navigational behavior and consequent mortality. Because chronic exposure to DA is widespread in CSLs, these impairments could have population-level consequences, particularly in combination with changing ocean conditions that lead to less reliable foraging conditions (*7*, *19*). In addition, these findings have practical application in the veterinary and rehabilitation setting. Given the negative correlation that we found between navigational memory and the extent of hippocampal damage, in vivo measurements of hippocampal volume in stranded sea lions may be useful markers of prognosis and postrelease outcomes. Specifically, animals with right dorsal hippocampal lesions might be at increased risk in the wild. More generally, these results, obtained from an ecologically valid sample of wild animals that were naturally exposed to DA, may be applicable to other affected species, including sea birds and cetaceans, that are less accessible for neurobehavioral study.

REFERENCES AND NOTES

1. C. A. Scholin *et al.*, *Nature* **403**, 80–84 (2000).
2. M. W. Silver *et al.*, *Proc. Natl. Acad. Sci. U.S.A.* **107**, 20762–20767 (2010).
3. T. Goldstein *et al.*, *Proc. Biol. Sci.* **275**, 267–276 (2008).
4. P. A. Silvagni, L. J. Lowenstine, T. Spraker, T. P. Lipscomb, F. M. D. Gulland, *Vet. Pathol.* **42**, 184–191 (2005).
5. J. O'Keefe, "Nobel lecture: Spatial cells in the hippocampal formation" (Nobel Media AB, 2014); www.nobelprize.org/nobel_prizes/medicine/laureates/2014/okeefe-lecture.html.
6. N. J. Fortin, K. L. Agster, H. B. Eichenbaum, *Nat. Neurosci.* **5**, 458–462 (2002).
7. M. J. Weise, D. P. Costa, R. M. Kudela, *Geophys. Res. Lett.* **33**, L22S10 (2006).
8. K. Thomas, J. T. Harvey, T. Goldstein, J. Barakos, F. M. D. Gulland, *Mar. Mamm. Sci.* **26**, 36–52 (2010).
9. Materials and methods are available as supplementary materials on *Science* Online.
10. V. D. Bohbot *et al.*, *Neuropsychologia* **36**, 1217–1238 (1998).
11. M. B. Moser, E. I. Moser, *Hippocampus* **8**, 608–619 (1998).
12. W. W. Roberts, W. N. Dember, M. Brodwick, *J. Comp. Physiol. Psychol.* **55**, 695–700 (1962).
13. S. B. Floresco, J. K. Seamans, A. G. Phillips, *J. Neurosci.* **17**, 1880–1890 (1997).
14. H. Eichenbaum, *Nat. Rev. Neurosci.* **1**, 41–50 (2000).
15. D. S. Olton, J. A. Walker, F. H. Gage, *Brain Res.* **139**, 295–308 (1978).
16. J. M. Parent *et al.*, *J. Neurosci.* **17**, 3727–3738 (1997).
17. B. Biswal, F. Z. Yetkin, V. M. Haughton, J. S. Hyde, *Magn. Reson. Med.* **34**, 537–541 (1995).
18. O. I. Lyamin, I. S. Chetyrbok, *Neurosci. Lett.* **143**, 263–266 (1992).
19. S. C. Doney *et al.*, *Ann. Rev. Mar. Sci.* **4**, 11–37 (2012).

ACKNOWLEDGMENTS

This research was conducted under authorization granted to the Marine Mammal Health and Stranding Response Program by the National Marine Fisheries Service under scientific research permit 932-1489-10, and it has been approved by the Institutional Animal Care and Use Committees at the University of California–Santa Cruz (UCSC) and The Marine Mammal Center (TMMC). We thank D. Casper and staff members at both UCSC's Pinniped Laboratory and TMMC for contributions to data acquisition and logistical support. Behavioral data are in the supplementary materials; imaging data are archived on Dryad at http://dx.doi.org/10.5061/dryad.0279k. None of the authors claim any competing financial interests.

SUPPLEMENTARY MATERIALS

www.sciencemag.org/content/350/6267/1545/suppl/DC1
Materials and Methods
Supplementary Text
Figs. S1 to S5
Tables S1 to S5
References (*20*–*23*)
Movies S1 to S3

13 May 2015; accepted 9 November 2015
Published online 14 December 2015
10.1126/science.aac5675

Algal toxin impairs sea lion memory and hippocampal connectivity, with implications for strandings

Peter F. Cook *et al.*

Science **350**, 1545 (2015);
DOI: 10.1126/science.aac5675

www.sciencemag.org/cgi/content/full/science.aac5675/DC1

Supplementary Materials for

Algal toxin impairs sea lion memory and hippocampal connectivity, with implications for strandings

Peter F. Cook,* Colleen Reichmuth, Andrew A. Rouse, Laura A. Libby, Sophie E. Dennison, Owen T. Carmichael, Kris T. Kruse-Elliott, Josh Bloom, Baljeet Singh, Vanessa A. Fravel, Lorraine Barbosa, Jim J. Stuppino, William G. Van Bonn, Frances M. D. Gulland, Charan Ranganath

*Corresponding author. E-mail: pfcook@emory.edu

Published 14 December 2015 on *Science* Express
DOI: 10.1126/science.aac5675

This PDF file includes:

Other Supplementary Material for this manuscript includes the following:
(available at www.sciencemag.org/cgi/content/full/science.aac5675/DC1)

Materials and Methods

Subjects

Subjects were 41 wild California sea lions (CSLs) selected from a larger population of individuals undergoing rehabilitation at The Marine Mammal Center (TMMC) in Sausalito, CA (Tables S1, S2). Age and sex were not controlled—due to demographics of stranded sea lions in central California, the majority of subjects were adult females. A sample size of 30 individuals was determined *a priori* for direct comparisons of performance on behavioral tasks to hippocampal volumes determined from brain imaging. Target sample size was based both on a power analysis (correlation: $r = 0.3$, $p = 0.05$, power = 0.3, $n = 23$) and the number of animals it was deemed feasible to evaluate during the three years allotted for the study. Participants were identified for the primary study by one veterinarian at TMMC (F. Gulland) who was instructed to select 20 CSLs suspected of domoic acid (DA) toxicosis and 10 without apparent neurological symptoms. Diagnoses were based on the criteria for chronic DA toxicosis defined by Goldstein et al., 2008 (*3*), which are dependent on evidence of hippocampal atrophy and intermittent seizures. Researchers remained blind to the veterinary assessment of each individual throughout the study, and the assessing veterinarian was blind to specific hypotheses to be tested. Of note, although direct measures of DA in tissue or body fluid were available for some animals, these are not a component of diagnosis for chronic DA toxicosis. This is for two reasons: 1) DA has a short half-life, and clears the body within 48 hours, and 2) chronic DA toxicosis is believed to be the result of prior exposure or exposures, not an acute manifestation of initial exposure (*3*). Because exposure history of wild animals is unknown, diagnosis of chronic DA toxicosis is not conclusive. However, the diagnostic criteria are supported by a robust body of research. Extensive histological screening of sea lions that die in captivity has strongly linked chronic exposure to specific hippocampal lesions. In addition, in over 1,000 stranded sea lions screened by MRI, toxicology or histology at TMMC in recent years, no other environmental exposure has been reliably linked with hippocampal damage. Hippocampal damage in this population is present in nearly all sea lions with chronic DA toxicosis, and is considered a sufficient symptom for diagnosis. (*1 ,3, 4*). Secondary selection criteria required that study animals be able to move effectively both on land and in water, be eating reliably unassisted, and be medically stable, as assessed by TMMC veterinary staff. Because they were drawn from a rehabilitation population, the apparent non-DA cases presented with a range of physical afflictions, including traumatic injuries, infections, malnutrition, and cancers (as described in this population in Grieg et al., 2005) (*20*). Following completion of the primary study, a second group of 11 animals was opportunistically selected for structural and functional MRI (fMRI), and took no part in behavioral testing. Access to the functional imaging suite was limited to 90 days, and data were acquired from as many subjects as were available and required diagnostic imaging for suspected neurological pathology or physical pathology (primarily trauma and carcinoma) during this period.

The 30 sea lions that participated in the primary study were individually and temporarily transported to Long Marine Laboratory at the University of California Santa Cruz (UCSC) for approximately 14 continuous days of behavioral research between April 2009 and November 2011. At the conclusion of behavioral testing, each animal underwent structural MRI at AnimalScan Advanced Veterinary Imaging Center in

Redwood City, CA. All 30 individuals completed testing in the delayed alternation task (described below). Twenty-six of these individuals also completed testing in the once-daily foraging task (described below)—the other four were unwilling to approach a baited location and take fish from it, even after repeated exposures, so were excluded from further testing. The 11additional animals that did not take part in behavioral testing, but did undergo structural and functional MRI, were imaged at the AnimalScan Imaging Center between August and October of 2012. The 41 sea lions that were involved in the project were returned to TMMC for further rehabilitation, assessment, and, if warranted, release into the wild immediately upon their individual completion of scheduled research.

Experimental Blinding

Strict procedures for experimental blinding were established prior to the start of the study. As the study design required comparisons between subjective veterinary status, volumetric measures of brain damage, and behavioral performance measures, it was essential that information from any one of these categories could not affect data collection in the others. Veterinarians selected subjects prior to collection of behavioral and imaging data, and was blind to all behavioral and volumetric data when assigning diagnoses; behavioral coders were blind to volumetric brain data and veterinary diagnoses; and volumetric tracers were blind to animal identity, behavioral data, and veterinary diagnoses. These three categories of data—veterinary, behavioral, and volumetric—remained segregated until the final stages of analysis, when they were unblinded and directly compared to assess experimental hypotheses.

Because it was essential that veterinarians provide an appropriate subject pool, it was not possible that they be fully blind to the general aim of the study, i.e., to identify the connection between brain damage and behavioral changes. However, the veterinarians were not informed of the explicit hypotheses to be tested. In addition, all behavioral and volumetric data were collected and computed after animal selection. Veterinarians remained unaware of any specific findings during the course of data collection. *Post-hoc* veterinary diagnosis was used as an independent measure in some analyses. This diagnosis was made following final disposition of each subject by a highly experienced veterinarian (F. Gulland). The information available included the brain scans and associated descriptive commentary from standard radiology review of the images, which is commonly used in diagnosis of DA toxicosis (*3*). Neither the diagnosing veterinarian nor the veterinary radiologist had access to behavioral or volumetric data on any animal during assessment and diagnosis.

The behavioral tests were conducted by individuals familiar with the study aims but blind to subject status. The data were coded *post-hoc* from video recordings by two individuals blind to veterinary assessment and volumetric data. These individuals were broadly familiar with the aims of the study in re comparing veterinary diagnosis and brain damage to behavioral measures. In some behavioral experimental designs, it is important that the coders be blind to the aims of the experiment. For example, if there are two experimental conditions, and the hypothesis is that all animals will react differently in these two conditions, awareness of the study aims could clearly bias data collection. In our study, there were no hypotheses that all animals would react in a particular way in a particular condition. Rather, the hypothesis was that behavioral impairment would correlate with volumetric measures of brain damage.

The volumetric brain data were coded on all 41 animals by one tracer who was not blind to study aims. Interobserver reliability was computed with tracings on a subset of these animals by a second tracer who, although aware that the study involved looking at brain damage in sea lions, was not informed of the specific experimental aims in regard to comparing brain damage and behavioral tests. Importantly, each tracer was fully blind to animal identity, veterinary assessment, and behavioral data when tracing. Each set of brain scans was coded with a randomly selected number by a third party, and all tracing and data computation was conducted using these codes. It is not uncommon in certain types of image analysis to blind the coder to all study aims. For instance, when assessing diagnostic images for signs of cancer, false positives may be higher when the assessing party is aware that the subjects are predisposed to cancer. Such a factor could theoretically have affected our study, as both tracers were aware that the study dealt with hippocampal lesions. However, because the comparisons of interest were with veterinary diagnoses and behavioral measures, a general tendency toward false positives (in this case, tracing in a manner that might reduce measured volume) would not bias the analysis. If all hippocampi were under-measured, this would be true for animals with larger and smaller hippocampi, and comparisons with veterinary diagnosis and behavioral measures would still be valid.

Functional MRI analysis to assess resting state connectivity was conducted by the same individual who served as the primary coder for volumetric brain data. As was the case for volumetrics, functional data for these 11 animals were assigned arbitrary codes, independent from coding assigned to trace and compute volumetrics. All image preprocessing and analysis was conducted using this code, such that the individual conducting analyses was unaware of animal identity, veterinary assessment, and volumetric measures during analysis. The data were unmasked only at the final stage of analysis for direct comparison with volumetric measures of hippocampal damage.

Behavioral Testing

General Procedure: Two behavioral procedures were conducted at Long Marine Laboratory: a short-term, delayed alternation task, and a once-daily spatial foraging task. All training and testing took place in the animal's home enclosure, which was a 10 m diameter by 2.5 m high circular area containing a 2 m diameter by 0.8 m high circular seawater pool with a broad ramp leading down to the floor of the enclosure. Reward used in behavioral training and testing was fish (either freshly thawed herring or capelin). Because subjects were undergoing active rehabilitation, and were potential candidates for release to the wild, all testing was conducted without direct human contact. Experimenters remained out of view during behavioral trials including when fish reward was delivered. All sessions were recorded and data were subsequently coded from video footage.

Delayed Alternation Task

In this procedure, the sea lions were required to navigate a two-choice maze (Fig. S2) requiring left and right alternation on subsequent trials.

Pre-training: Initial training for the delayed alternation task began for each animal on the first day at the laboratory, and proceeded as follows, with some small degree of variability. First, subjects were trained to repeatedly leave the small pool and walk down

the ramp to the deck, returning each time to the pool to start again. This was done first through baiting, and then through successive approximation using fish reward. During training and testing sessions, the experimenter dispensed fish by throwing it into the pen from behind a blind, on deck above the enclosure. All fish rewards were paired with a brief whistle, which served as a conditioned reinforcer.

When the subject was reliably walking down the ramp to the deck to receive fish reward without requiring any baiting (this generally required 2–3 training sessions), the next phase of training began. In this phase, the maze was put in place. The maze was a 2.4-meter-long wooden chute, 1.5 meters in height, that, when placed for training and testing sessions, extended directly from the end of the ramp descending from the subjects' pool. At the end of the chute on either side were two pairs of hinged saloon doors, one pair on the left, one on the right. These opened outward such that an animal exiting via one of them would be moving perpendicularly to the body of the maze's chute. There were no return arms leading back from these doors to the beginning of the maze. Baiting was used to prompt the animal to enter the maze from the pool and exit via one of the sets of doors. During initial training, the animal was baited through the maze and out the doors in an alternating pattern on successive trials—the "correct" set of doors was also held open and the "incorrect" set of doors was held closed via a remote mechanism on each trial, such that each animal received balanced reinforcement history with each door during initial training.

When the subject was reliably moving through the maze in this manner without any baiting required, the experimenter began opening the target doors slightly less on each successive trip through the maze (or "trial"), such that the animal began to have to actively push through the door to fully exit the maze. There was some variability in how long this phase extended, primarily dependent on how willing an animal was to push through the partially opened doors. When the subject was finally pushing through fully closed doors on both sides, the next phase of training began.

No-delay alternation: In this phase, the experimenter no longer provided direct guidance to the animal to influence decisions about which door to use to exit the maze. Instead, the experimenter rewarded correct choices (marked by the conditioned reinforcer, followed by delivery of fish) and did not reward incorrect choices. A "correct" choice was defined as the first door selected on any particular session, regardless of which it was, and subsequently on each trial within a session, the door opposite of that most recently selected.

Two to four sessions of 20 trials were conducted each day. When performance reached 85% correct responses on two subsequent 20-trial sessions in the no-delay condition, subjects were acclimated to a gate at the head of the maze that could be remotely opened to block or enable access to the maze on successive trials; during acclimation the delay interval was gradually increased from one to seven seconds.

Delay testing: For the test condition, subjects received 40 trials using a forced 7-s delay and, in subsequent testing sessions, 40 similar trials using a 20-s delay. These test sessions were conducted in matched pairs of 10 delay and 10 no-delay trials so final performance could be compared against the baseline (no delay) condition.

All subjects met the 85% performance criterion on baseline trials within 700 training trials (counted including initial trials with baiting, mean: 326 trials, standard deviation: 131 trials, Table S3). Neither right nor left hippocampal volume predicted number of

trials required to reach criterion (right: $t(0.43) < 1$, $df = 27$; left: $t(0.00) < 1$, $df = 27$, Table S3), and performance on no-delay test trials was not predicted by right or left hippocampal volume (right: $t = 1.17$, $df = 27$, $p = 0.25$; left: $t(0.43) < 1$, $df = 27$). This indicates that baseline performance on the alternation task was unaffected by brain damage, and justifies use of performance on delay trials as a dependent variable representing task-specific memory.

Because mean group performance on the 20-second delay tests was below chance (17/40 correct trials, Table S3), with only 6 of 30 animals performing above chance (> 20/40 correct trials), the task was judged too difficult given the limited training history of these wild subjects, and data from these trials were disregarded for further analysis. In contrast, mean performance on 7-s delay trials was 23/40, with 20 out of the 30 animals performing above chance.

Once-Daily Foraging Task

In this test, four potential food locations (identical opaque plastic buckets) were lowered simultaneously via a system of ropes and pulleys into the animal's enclosure (Fig. S3) once per day. The four locations were set roughly equidistant from the pool, and did not change within or across subjects. Once lowered, buckets were arrayed along the external wall of the large holding pool, with 3.7 m separating each bucket. For each subject, one—and only one—of the locations contained fish across all testing days. The baited location was randomized across subjects. The amount of fish used in each exposure varied with animal size and appetite, but was set at approximately a sixth of the animal's daily diet, so as to constitute a salient reward. Each bucket was marked with fish scent prior to each presentation to control for the possibility of olfactory cuing. The inside of the buckets were not visible to the subjects until they had drawn quite near. The buckets remained available until the subject had eaten all of the fish in the baited location and visited each of the buckets at least once, or until the subject had eaten all the fish and 5 minutes had passed from the initial point of presentation. The buckets were then lifted simultaneously from the pen.

To control the animal's beginning location, each presentation began after fish were thrown into the pool. The animal returned to the pool to consume the fish while the buckets were lowered into the enclosure. In this way, a subject's relative distance to each of the four food locations at the beginning of a testing session was held roughly constant across testing, but their position within the pool and body orientation were variable.

Pre-training: Animals were hesitant to approach and consume fish from buckets during pilot work, so a familiarization phase was implemented prior to testing. During the first three days at the laboratory, each sea lion was presented on multiple occasions with a single bucket—identical to the buckets used in the subsequent testing—baited with fish. These presentations occurred at a neutral location, on the opposite side of the enclosure from and equidistant to the four test locations. If subjects did not approach and explore the bucket of their own volition they were prompted to do so through baiting—that is, fish were dropped from a concealed location into the bucket until the subject investigated. This training was conducted between 1–3 times per day, dependent on a subject's predilection for approaching the bucket and finding the fish reward. Four of the 30 subjects taking part in behavioral testing showed aversion to the bucket and would not reliably approach, even after three days of pre-training. These animals were excluded

from further testing in the foraging task. Testing began at the end of the first day in which the animal first approached the training bucket and found and consumed the fish without prompting. Despite this training, prompting a response to the buckets during the first few test presentations of the buckets was sometimes required (mean number of trials with prompting = 1.54; standard deviation = 0.90; 28 subjects required no more than 2 days of prompting (the exceptions required 3 and 4 respectively)). Prompting was accomplished by remotely raising and lowering all buckets repeatedly and simultaneously to draw attention. In most cases, this was adequate to trigger exploration. If not, the subject was baited to each location in turn by fish thrown next to each bucket location in random order. Such baiting was only ever implemented on the first day of testing, and data from sessions using prompting and/or baiting were not used in subsequent analyses. Number of sessions requiring prompting or baiting was not correlated with either dependent measure drawn from this behavioral test, justifying the use of these dependent measures in regression analyses with hippocampal volumes (within-session errors: $F = 0.24$, $R^2 = 0.01$, $p = 0.63$; Cross-session acquisition: $F = 0.05$, $R^2 = 0.00$, $p = 0.82$).

Structural Brain Imaging

Brain imaging, both structural and functional, was conducted at the AnimalScan Advanced Veterinary Imaging facility in Redwood City, CA, on a 1.5 T Siemens Magnetom Symphony scanner. All animals were imaged *in vivo* while under isoflurane anesthesia with direct veterinary supervision. Many of the animals were pre-medicated with a combination of midazolam (0.1mg/kg), butorphanol (0.15mg/kg) and/or medetomidine (0.035 mg/kg) intramuscularly injected in order to facilitate the mask induction with isoflurane. The medetomidine was reversed with an equal volume of atipamezole given intramuscularly once the animal was taken off of isoflurane anesthesia. During scanning, animals' heads were positioned in a CP extremity coil, selected to optimize signal-to-noise ratio.

Structural MRI: To obtain measures of hippocampal volume, each subject (n = 41) in this study underwent structural MRI. Turbo Spin Echo (TSE) T2-weighted scans were obtained in an oblique plane perpendicular to the longitudinal axis of the hippocampus. This protocol was directly based on prior work on sea lion hippocampal volumetrics (*21*).

Two protocols were used for structural imaging—one for the 30 animals who took part in behavioral testing (TR = 5470 ms, TE = 14 ms, FOV = 160 x 160 mm, slice thickness = 2.0 mm, voxel size = 0.625 mm x 0.695 mm x 2 mm), and the other for the 11 additional animals who took part in the fMRI study (TR = 3950 ms, TE = 98.0 ms, FOV = 160 x 160 mm, slice thickness = 3.3 mm, voxel size = 1.25 mm x 1.25 mm x 3.3 mm). The greater slice thickness for the animals taking part in fMRI was necessary to keep overall scan time down; to reduce potential complications with anesthesia, total scan time was kept under an hour.

Volumetric Morphometry: For each subject, left and right hippocampal volume was characterized as a ratio over total brain volume (minus the cerebellum). Using a measure of hippocampal volume relative to total brain volume helps to control for natural variation in hippocampal volume as a function of natural variation in brain size, irrespective of any neuropathology. To determine volumes, manual tracing was conducted using Quanta2 software (UC Davis IDEA Lab, Alzheimer's Disease Center

grant, NIH P30 AG010129). Tracing for all 41 animals was conducted according to the criteria described below.

For volumetric morphometry, images were acquired in a plane perpendicular to the septo-temporal (longitudinal) axis of the hippocampus (Fig. S1) following the protocol used in prior studies delineating sea lion hippocampus (*21*). This protocol includes tracing on T2-weighted images, as this produces excellent image contrast between the lateral and caudoventral boundaries of the hippocampus and cerebrospinal fluid (CSF) surrounding the cornu ammonis (CA). We identified hippocampal structures as in Montie et al., 2009 (*21*), and these were cross-checked by a veterinary radiologist (S. Dennison) and research veterinarian (F. Gulland), both highly experienced in examining marine mammal brains, and with experts in human hippocampal neuroimaging (C. Ranganath, O. Carmichael).

Complete hippocampal tracings included the CA, alveus, and dentate gyrus. A portion of the subiculum was also included. As noted by Montie et al., 2009 (*21*), at this imaging resolution there are no reliable landmarks to establish a clear boundary between CA and subiculum.

Septal and temporal boundaries for hippocampal tracing were based on those used previously (*21*), and were conservative, privileging replicability over inclusion of all potential hippocampal tissue.

The septal-most slice on which hippocampus was traced was that immediately ventral to the splenium of the corpus callosum (Fig. S1B). In this plane, the rostral (but not caudal) colliculi are plainly visible, and the hippocampus assumes a "flattened" aspect as in primates. Sea lion hippocampus is grossly similar to that seen in primates, and unlike that of rodents and some carnivores, does not show a large rostral protrusion at the septal terminus. Hippocampal tissue dorsal to the ventral boundary of the splenium is neglible.

The temporal-most slice on which hippocampus was traced was that in which the cerebral peduncles were clearly visible along with the interpeduncular fossa (Fig. S1I). Although there is hippocampal tissue rostroventral to this plane, the temporal-most portion of the hippocampal head is difficult to differentiate from the amygdala at the imaging resolution we used, so was excluded from tracing.

Lateral boundaries of the hippocampus on all slices were defined by the lateral ventricle of the temporal horn. Tracings included the alveus but excluded the fimbria.

Medial boundaries of the hippocampus on all slices were defined by the medial-most extension of the subicular cortex, clearly visible in contrast to the temporal recess.

Ventral boundaries of the hippocampus on each slice followed subiculum, CA and alveus dorsal to the parahippocampal gyrus. Rostroventrally, the ventral boundary was defined by a straight line connecting the medial-most portion of subicular cortex to the medial-most point of parahippocampal white matter dorsal to the parahippocampal gyrus.

Dorsal boundaries of the hippocampus on each slice followed the subicular cortex and CA, excluding the hippocampal sulcus and fimbria. On rostroventral slices, this boundary was clearly delineated by the temporal recess. On caudodorsal slices, portions of the boundary were apparently flush with, but clearly delineated by, the caudal boundary of the pulvinar of the thalamus.

Tracing Reliability Measures: Intra-comparison correlations were computed between the hippocampal volumes measured by the primary tracer who evaluated all

study animals (n=41) and those measured by a secondary, independent tracer who evaluated a random subset of the study animals (n=10) (right hippocampus: $r = 0.838$, $p < 0.0001$; left hippocampus: $r = 0.904$, $p < 0.0001$). These correlations show high agreement between the two independent raters, and therefore high reliability in the tracing protocol. In addition, across the 30 animals used in behavioral testing, right (mean = 0.18%, standard deviation = 0.04%) and left hippocampal volume (mean: 0.19%, sd: 0.04%) were not distinct ($t(0.87) < 1$, $df = 58$), justifying their use as separate independent variables in regression analyses with behavioral measures.

Dorsal and Ventral Hippocampal Division: Hippocampal tissue was further segregated into dorsal and ventral portions for follow-up analyses. Because there were no prior data on functional division along the longitudinal axis of the CSL hippocampus, we adopted the conservative approach of dividing the hippocampi in half by length, and it was these values (Table S1) that were used in the analyses reported in the paper. To obtain volume measures for ventral and dorsal hippocampus, masks for total left and right hippocampus were divided exactly in half for hippocampi with an even number of slices. For hippocampi with an odd number of slices, the volume of the middle slice was divided evenly and split between the volume of the remaining ventral and dorsal slices.

Of note, rodent data suggest the dorsal third of the hippocampus is sufficient for supporting spatial memory (*11*). While CSL and rodent hippocampal anatomy is grossly different—with the rodent hippocampus showing a large rostrodorsal extension in comparison to the flattened caudodorsal terminus of the CSL hippocampus—we believed data on the dorsal third of the CSL hippocampus by length would provide an interesting comparison to rodent data, and potentially a further validation of our findings. Therefore, in comparisons where the dorsal half of the right hippocampus was a significant predictor of behavior, we repeated the dorsal/ventral regression analyses using the volume of the dorsal third of the right hippocampus (Supplementary Text).

Functional Connectivity Brain Imaging

Resting state functional connectivity MRI was conducted on eleven subjects following the primary study. The same anesthesia protocol detailed above for structural imaging was used. Fifteen minutes of fMRI data were acquired in the transverse plane for each subject using a standard BOLD sequence (single shot echo-planar imaging (EPI), 90 degree flip angle, TR = 2.5 s, TE = 40 ms, voxel size = 3mm x 1.25 x 1.25).

The resultant BOLD time series was preprocessed using FSL's (*22*) FEAT, including motion correction, slice-timing correction, and band-pass filtering (0.01 Hz–0.1 Hz), and excluding spatial smoothing. Motion parameters were temporally filtered at the same bandwidth as the BOLD time series in MATLAB for inclusion in functional connectivity models.

To control for non-specific physiological noise in the brain, probabilistic white matter and CSF masks were generated for each subject using FSL's FAST, and thresholded at $p(\text{tissue}) > 0.95$.

In order to measure functional connectivity (*17*) between the hippocampi and the rostrodorsal thalamus, masks of these structures were created. Left and right hippocampal masks were drawn directly on each subject's structural scan with the same anatomical criteria used for volumetric tracing. Left and right rostrodorsal thalamic masks were manually drawn on a high-resolution (1 mm isotropic) diffusion-weighted steady-state

free precession (DW-SSFP) scan **(**Fig. S4**).** This scan was obtained on a 3T Siemens Trio scanner opportunistically from a post-mortem brain of a wild sea lion with no apparent neurological symptoms. This animal was euthanized due to advanced neoplasia following four days in rehabilitation and received a post-hoc diagnosis of carcinoma. The brain tissue was subsequently sectioned and evaluated by a veterinary pathologist naïve to study aims, and no evidence of brain pathology was found in the hippocampus or any other structure. Parameters for the DW-SSFP sequence were as follows: 52 directions, FOV = 166 mm, voxel size = 1 mm isotropic, TR = 31 ms, TE = 24 ms, flip angle = 29°, bandwidth = 159 Hz/pixel, q = 10 cm -1, Gmax = 38.0 mT/m, gradient duration = 15.76 ms. The lateral and ventral boundaries of the masks were in line with the lateral and ventral boundaries of the head of the caudate nucleus. The caudal boundaries were in line with the rostral bank of the left and right insula. Prior work has not segmented the sea lion thalamus, but nuclear boundaries were clearly visible on the B0 image, and were drawn in keeping with data on hippocampal-thalamic projections and thalamic segmentation in other carnivores (dorsal to the medial nuclei and rostral to the medial and dorsolateral nuclei) (*23*).

All anatomical masks were back-registered into native functional space with FSL's FLIRT. BOLD time courses averaged across voxels were extracted for left and right hippocampal and rostrodorsal thalamic regions at the individual subject level. Correlation coefficients between time courses were used as measures of functional connectivity at the individual subject level (17*)*.

For comparison of functional connectivity in animals with DA toxicosis and those without, subjects were sorted into two groups based on hippocampal volume. Five of the eleven animals had relative right or left hippocampal volume > 1 SD lower than group means drawn from all 41 animals across both phases of the present study (Tables S1 & S2), and were assumed to have DA-induced brain damage. The other six animals showed no signs of brain lesion per volumetrics or assessment by a veterinary radiologist, and showed no neurological symptoms per veterinary diagnosis, so were used as a provisional control group. In addition to the repeated measures ANOVA reported in the main text, planned post-hoc t-tests were conducted comparing functional connectivity between the individual left and right hippocampal and thalamic seeds (Supplementary Text).

A follow-up, voxelwise analysis was conducted on the six control animals to assess hippocampal-thalamic connectivity. For each of the six subjects, two functional connectivity analyses were performed in FEAT using the general linear model (GLM), one each for left and right hippocampus. Preprocessing parameters were identical to those described above, with the addition of spatial smoothing with a 5 mm Gaussian kernel. Separately for each hippocampal mask (left and right), a GLM was set up with the hippocampal timecourse as the covariate of interest and white matter and CSF timecourses, as well as motion parameters (temporally filtered at the same frequency as the BOLD timeseries) as nuisance covariates (i.e., to control for variance in the data due to motion artifacts and physiological changes as opposed to actual neural signal).

Functional connectivity GLMs generated two whole-brain functional connectivity images for each subject estimating the correspondence between the timecourse of each hippocampal seed with all other voxels in the brain. In preparation for voxelwise group analysis, these native-space functional connectivity images were first co-registered to co-planar high-resolution structural images (6 degrees of freedom (DOF)) and then

normalized to a template brain produced by co-registering the 11 study subjects' high-resolution structural images (12 DOF) with FSL's FLIRT.

For each of the two hippocampal seeds, a voxelwise group connectivity map was generated across the six control animals based on a one-sample t-test in FEAT. The region of highest bilateral activation (thresholded at $p < 0.01$) was the rostrodorsal thalamus (Fig. S5). This finding of high hippocampal-thalamic functional connectivity in the control animals further justifies focusing on connectivity between these specific structures for the comparison between control animals and those with apparent hippocampal damage.

Supplementary Text

Results

Hippocampal Dorsal Third Regression with Behavioral Measures: Findings with regression analyses using the volume of the dorsal third of the hippocampus were similar to those in the analyses using the dorsal half of the hippocampus (Table S4). In a regression with number of errors on 7-s delay trials as the dependent variable and volumes of dorsal third and ventral half of the right hippocampus and number of errors on no-delay test trials as independent variables, the dorsal third of the right hippocampus was a marginal predictor of performance in the delayed alternation task ($t = -1.75$, $df = 26$, $p < 0.1$). In this regression analysis, as in that using the dorsal half, the volume of the ventral half of the right hippocampus did not predict behavioral performance ($t = 0.13$, $df = 26$, $p = 0.9$).

In a regression with learning rate in the foraging task as the dependent variable and the volumes of dorsal third of right and left and ventral half of right and left hippocampus as the independent variables, the dorsal third of the right hippocampus positively predicted acquisition rate ($t = -2.56$, $df = 1$, $p < 0.025$). The ventral half of the right hippocampus was a marginal negative predictor of acquisition rate ($t = 1.81$, $df = 21$, $p < 0.1$).

Functional Connectivity of Individual Hippocampal and Thalamic Regions: In planned post-hoc t-tests comparing functional connectivity of individual hippocampal and thalamic regions between animals with apparent hippocampal damage (n=5) and controls (n=6), all mean hippocampal-thalamic correlations were higher in the control than DA animals (right hippocampus to right thalamus: $t = -2.74$, $df = 9$, $p < 0.05$; right hippocampus to left thalamus: $t = -2.76$, $df = 9$, $p < 0.05$; left hippocampus to right thalamus: $t = -2.35$, $df = 9$, $p < 0.05$; left hippocampus to left thalamus: $t = -3.16$, $df = 9$, $p < 0.01$). Connectivity was also higher between right and left thalamus in the control animals ($t = -2.5$, $df = 9$, $p < 0.05$), indicating disruption of thalamic connectivity in DA animals.

Fig. S1.

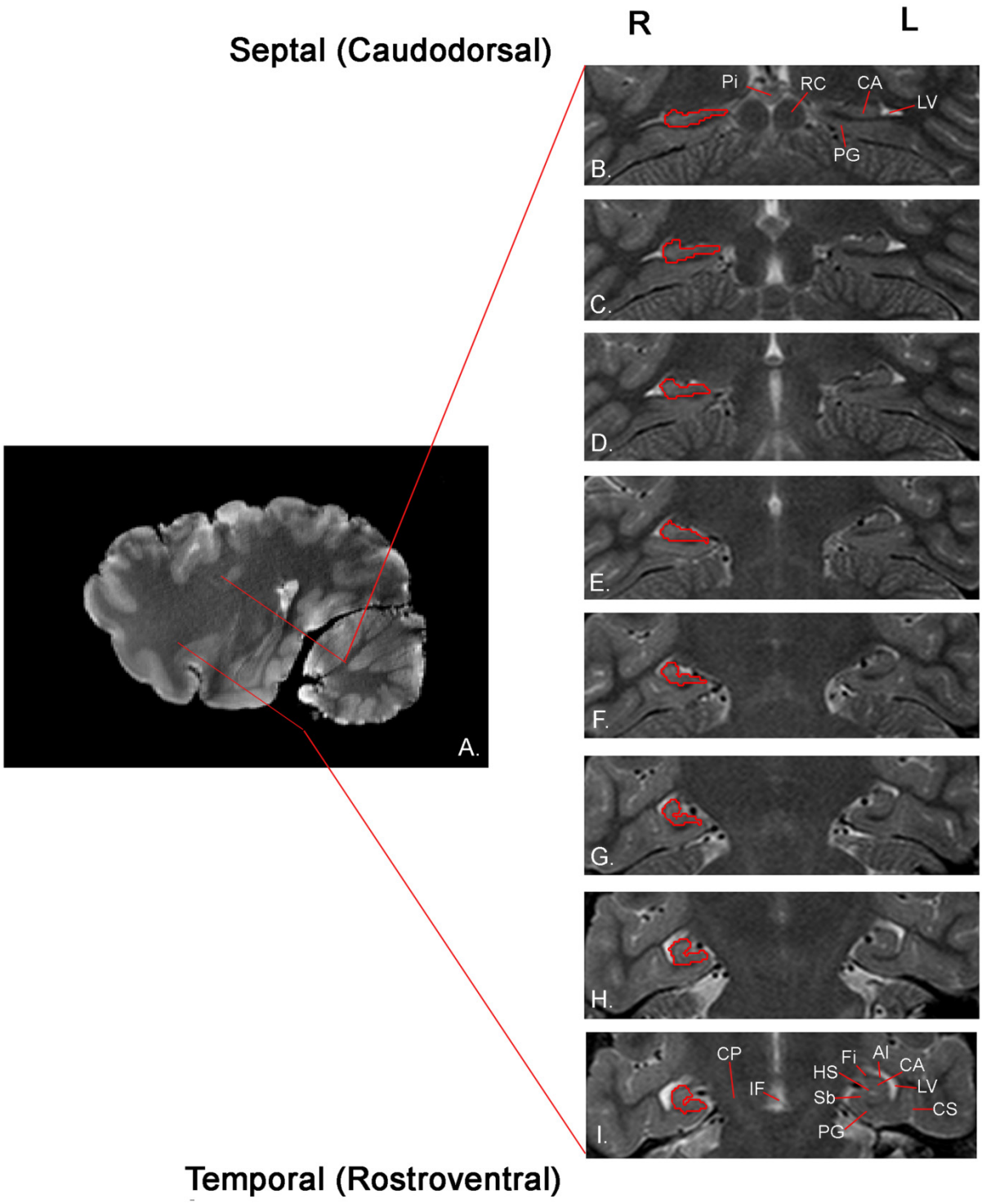
R
L
Septal (Caudodorsal)
Pi
RC
CA
LV
PG
B.
C.
D.
E.
F.
G.
H.
A.
CP
IF
Fi
Al
HS
CA
LV
Sb
CS
PG
I.
Temporal (Rostroventral)

Hippocampal Tracing: Representative T2-weighted image slices obtained along the transect indicated by the red lines. These show a complete right hippocampal tracing for one subject, represented on the left side of the individual slices (B through I from septal to temporal). Hippocampus was traced perpendicular to the septo-temporal axis (A), extending from the caudodorsal most slice, just inferior to the splenium (B) to the rostroventral most slice first clearly showing the cerebral peduncles and interpeduncular fossa (I). Tracings included CA, alveus, dentate gyrus and a portion of subiculum, and excluded the fimbria, hippocampal sulcus, and parahippocampal gyrus. Abbreviations: Al: alveus CA: cornu ammonis CP: cerebral peduncle CS: collateral sulcus Fi: fimbria IF: interpeduncular fossa HS: hippocampal sulcus LV: lateral ventricle of temporal horn PG: parahippocampal gyrus Pi: pineal gland RC: rostral colliculus Sb: subiculum

Fig. S2

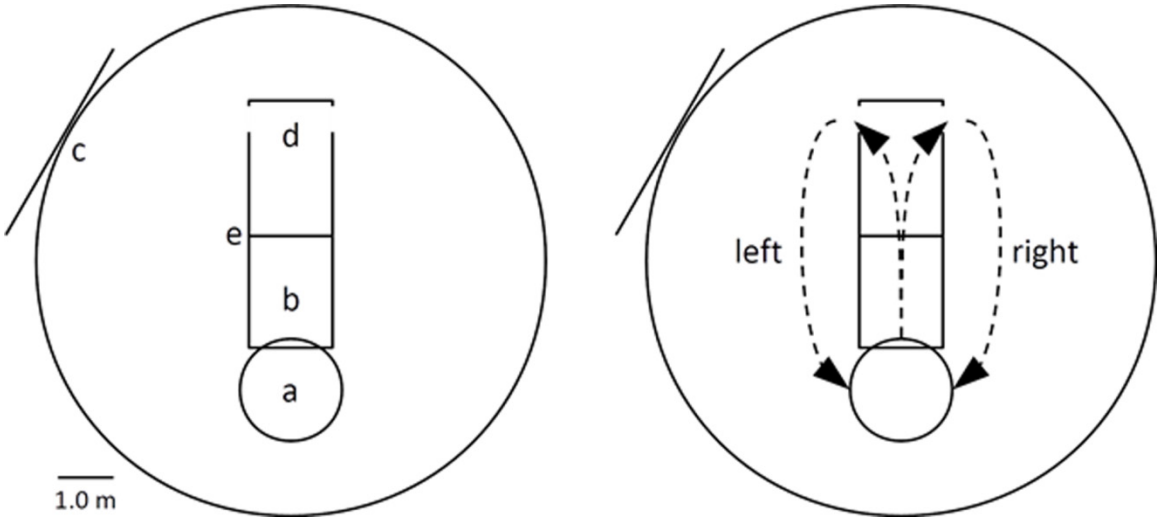

Delayed Alternation Test Schematic: A schematic representation of the two-choice maze used for delayed alternation testing. Shown relative to the circular enclosure that surrounded the living space of each subject is (a) pool, (b) ramp, (c) elevated blind from behind which all experiments conducted, (d), chute of maze, and (e) hinged gate for enforcing delay. The two potential trajectories (left and right) through the maze are shown via dashed lines in the right figure.

Fig. S3

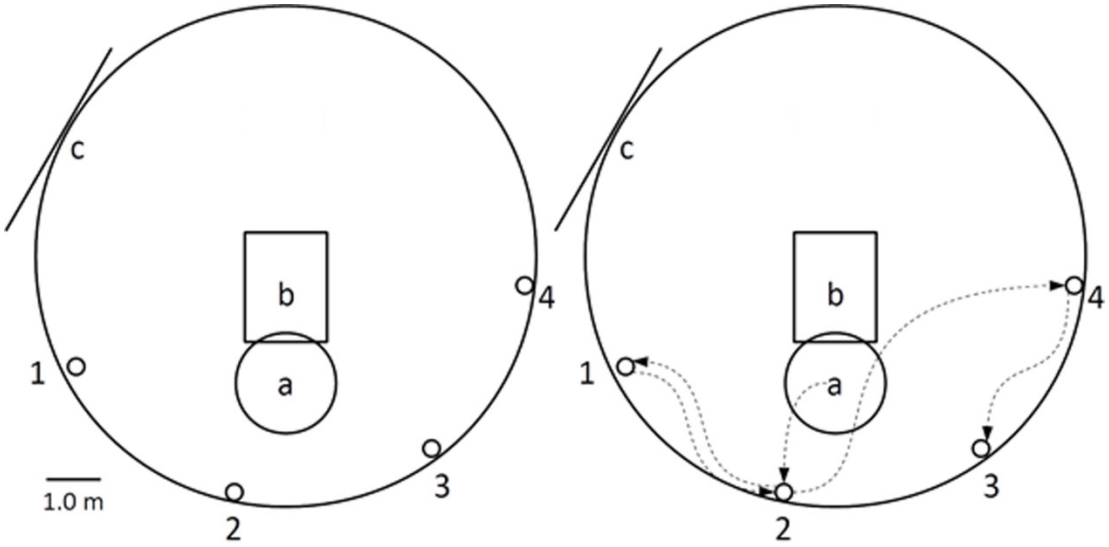

Once-Daily Foraging Test Schematic: A schematic of the testing setup for the once-daily foraging task. Shown relative to the circular enclosure that surrounded the living space of each subject are (a) pool, (b) ramp, and (c) blind. Numbers 1–4 indicate the locations where identical opaque buckets were presented, one of which always contained a predictable fish reward, its location randomized across subjects. A possible search trajectory is shown via dotted lines in the right figure.

Fig. S4

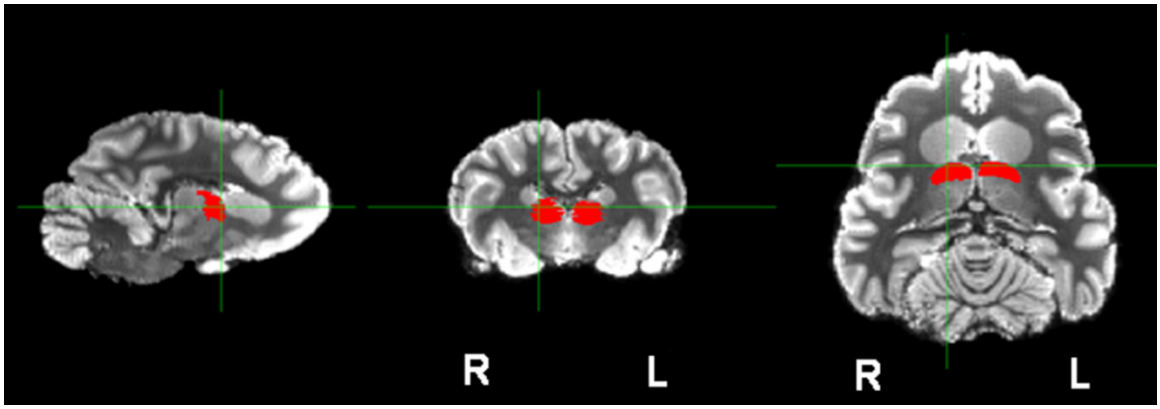

Anatomical Tracing of Rostrodorsal Thalamus: Separate left and right anatomically defined, rostrodorsal thalamic masks are shown in red in the sagittal (left), coronal (center), and transverse planes (right). The right thalamic mask is shown on the left and vice versa. These were drawn on images obtained post-mortem from an individual, healthy brain scanned at 1 mm isotropic resolution on a 3T Siemens Trio scanner.

Fig. S5.

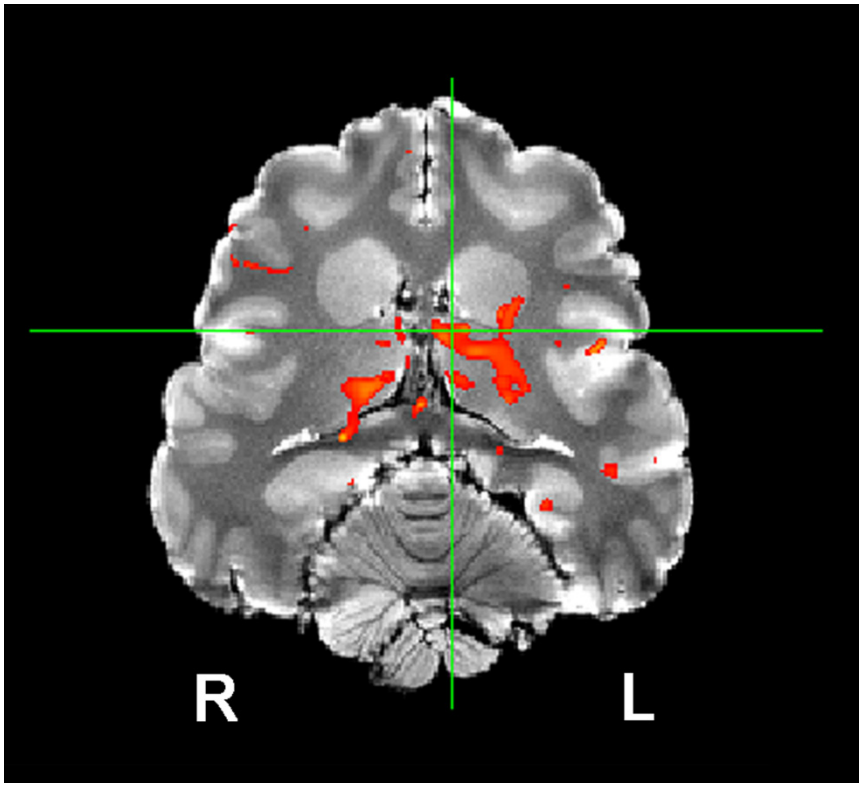

Voxel-Based Analysis of Hippocampal-Thalamic Connectivity in Controls: Combined voxel-based analysis maps of hippocampal connectivity in the 6 control animals are shown up-sampled into high-resolution (1 mm isotropic) structural space. Results from separate GLMs with the right hippocampus and left hippocampus as seed regions are superimposed. Regions showing high correlation with hippocampal seed timecoureses are shown in red and yellow and are thresholded at $p < 0.01$. Crosshairs are centered over the left rostrodorsal thalamus.

Table S1.

Study Phase 1 Diagnoses, Radiological Assessments, and Structural MRI Measures: Field identification number, veterinary diagnosis, radiologist assessment of hippocampal integrity (no damage: "no", right unilateral lesion: "rhp", left unilateral lesion: "lhp", or bilateral lesion: "bhp"), and hippocampal volumes (morphometric values as percentage of total brain volume for each region, including ventral: "v" and dorsal: "d") for each of the study subjects taking part in the behavioral tasks. Veterinary diagnosis was determined following final disposition of each patient, considering all patient information (including radiologist assessment), but independent of results of the present study. Radiologist assessment of hippocampal damage was done subjectively, based off of examination of high-resolution structural MR images, and blind to animal condition and status.

ID	Vet. Diagnosis	Rad.	Rhp	Lhp	vRhp	dRhp	vLhp	dLhp
8052	malnutirition	no	0.222	0.196	0.116	0.107	0.101	0.096
8095	malnutrition	no	0.263	0.239	0.120	0.143	0.113	0.126
8105	chronic DA	bhp	0.117	0.224	0.067	0.050	0.119	0.104
8684	mild acute DA	bhp	0.196	0.198	0.101	0.095	0.099	0.099
8181	malnutrition	bhp	0.224	0.174	0.111	0.113	0.082	0.091
8883	chronic DA	bhp	0.138	0.235	0.073	0.065	0.126	0.108
8722	chronic DA	bhp	0.125	0.224	0.073	0.052	0.123	0.101
9110	gas-bubble disease	no	0.231	0.207	0.120	0.112	0.116	0.092
8973	malnutrition	no	0.216	0.235	0.105	0.110	0.114	0.121
9325	chronic DA	rhp	0.152	0.220	0.076	0.077	0.104	0.115
9336	unknown	bhp	0.142	0.142	0.058	0.084	0.072	0.070
9364	trauma, malnutrition	no	0.243	0.206	0.127	0.116	0.113	0.093
9597	chronic DA	lhp	0.224	0.144	0.121	0.103	0.072	0.072
9679	chronic DA	rhp	0.184	0.237	0.099	0.085	0.114	0.123
9752	mild chronic DA	rhp	0.142	0.210	0.076	0.066	0.103	0.107
9690	chronic DA mild	lhp	0.219	0.167	0.110	0.110	0.081	0.086
9724	chronic DA	no	0.232	0.229	0.126	0.106	0.119	0.110
9807	chronic DA	rhp	0.123	0.211	0.052	0.071	0.111	0.100
9821	chronic DA	bhp	0.146	0.135	0.067	0.079	0.067	0.068
9866	chronic DA	bhp	0.215	0.182	0.119	0.096	0.090	0.092
9881	chronic DA	rhp	0.152	0.185	0.071	0.081	0.097	0.088
9923	DA	bhp	0.138	0.198	0.080	0.058	0.103	0.095
9931	chronic DA	bhp	0.166	0.116	0.081	0.085	0.058	0.057
9949	chronic DA	bhp	0.130	0.126	0.060	0.070	0.073	0.053
9988	normal	bhp	0.199	0.213	0.102	0.097	0.103	0.110
10091	chronic DA	bhp	0.117	0.108	0.062	0.055	0.056	0.052
10121	leptospirosis	rhp	0.230	0.219	0.115	0.115	0.114	0.105
10187	chronic DA	rhp	0.211	0.244	0.105	0.107	0.129	0.114
10170	gas-bubble disease	no	0.224	0.197	0.121	0.104	0.105	0.093
10235	trauma	bhp	0.215	0.192	0.120	0.096	0.099	0.093

Table S2.

Study Phase 2 Diagnoses, Radiological Assessments, and Structural and Functional MRI Measures: Field identification number, veterinary diagnosis, radiologist assessment of hippocampal integrity (no damage: "no", right unilateral lesion: "rhp", left unilateral lesion: "lhp", or bilateral lesion: "bhp"), hippocampal volumes (morphometric values as percentage of total brain volume for each region), and Z-scored correlation coefficients of BOLD time courses between hippocampal and thalamic masks for each of the subjects taking part in the functional imaging study (Rthal = right rostrodorsal thalamus, Lthal = left rostrodorsal thalamus). Veterinary diagnosis was determined following final disposition of each patient, considering all patient information (including radiologist assessment), but independent of results of the present study. Radiologist assessment of hippocampal damage was done subjectively, based off of examination of high-resolution structural MR images, and blind to animal condition and status.

ID	Vet. Diagnosis	Rad.	Rhp	Lhp	Z-Rhp-Lthal	Z-Rhp-Rthal	Z-Lhp-Lthal	Z-Lhp-Rthal
10371	trauma	no	0.194	0.209	0.008	-0.731	-0.451	-0.049
10376	carcinoma	no	0.098	0.161	-0.155	0.012	-0.132	-0.168
10392	trauma	no	0.23	0.219	-0.236	-0.153	-0.233	-0.210
10397	normal	bhp	0.19	0.165	-0.053	-0.035	0.030	0.217
10398	trauma	no	0.187	0.202	-0.071	-0.041	-0.056	-0.066
10402	mild acute DA	lhp	0.213	0.1	-0.153	-0.159	0.453	0.425
10413	leptospirosis	lhp	0.137	0.132	0.051	0.264	0.198	0.172
10421	chronic DA	no	0.127	0.173	0.483	0.297	0.781	0.571
10433	trauma	no	0.241	0.241	0.254	0.183	0.281	0.198
10434	leptospirosis	no	0.178	0.162	0.809	0.351	0.649	0.217
10437	leptospirosis	no	0.132	0.144	0.520	0.682	-0.056	0.013

Table S3.

Results of Behavioral Testing: Primary behavioral results from all subjects (designated by ID number). From the alternation ("Alt.") task: number of trials in the maze prior to meeting the testing criterion and errors during matched no-delay and delay testing trials for both the 7-s and 20-s delay tests. From the once-daily foraging task: mean within-session errors and the logged cross-session acquisition power curve. Day-by-day data for the foraging task are available for each subject in Table S5.

ID	Alt. Trials to Criterion	7s Alt. No-Delay Errors	7s Alt. Delay Errors	20s Alt. No-Delay Errors	20s Alt. Delay Errors	Foraging Errors	Foraging Acquisition
8052	421	8	3	NA	NA	1.55	-0.79
8095	363	15	18	NA	NA	1.14	-1.43
8105	434	10	20	NA	NA	5.00	-0.25
8684	283	10	19	22	26	2.29	-0.77
8181	107	15	23	13	28	1.20	-0.58
8883	312	8	18	6	21	6.36	-0.17
8722	321	12	33	14	27	1.89	-0.33
9110	696	5	17	13	21	0.67	-0.26
8973	195	6	9	5	10	NA	NA
9325	512	6	24	9	25	NA	NA
9336	270	4	12	9	20	NA	NA
9364	296	6	8	5	11	0.64	-0.42
9597	305	12	20	6	23	3.55	0.07
9679	285	5	16	16	28	2.75	-0.24
9752	326	6	9	5	39	1.75	-0.21
9690	351	7	12	4	24	1.50	-0.32
9724	287	10	17	16	19	1.09	-0.23
9807	201	12	30	14	27	0.75	-0.20
9821	159	8	14	6	22	1.88	-0.61
9866	231	8	28	9	26	2.67	-0.54
9881	186	6	18	9	25	3.13	-0.44
9923	327	4	20	6	23	1.30	-0.03
9931	509	3	23	11	28	1.00	-0.11
9949	249	6	16	5	8	3.43	-0.71
9988	237	8	10	8	14	1.17	-0.55
10091	420	7	26	8	26	2.88	-0.24
10121	302	7	9	4	15	1.00	-0.29
10187	306	4	12	6	26	1.80	-0.33
10170	632	20	23	12	16	1.20	-0.29
10235	265	6	19	10	24	NA	NA

Table S4.

Multiple Regression Results for Comparisons of Behavior and Hippocampal Damage: Multiple regression results for all primary comparisons of behavioral results against hippocampal volumes (Rhp = right hippocampus, Lhp = left hippocampus, v = ventral half, d = dorsal half). Hippocampal volumes were used as independent variables, and behavioral measures as dependent variables. For the delayed alternation tasks, number of errors on the 7-s delay test was used as the dependent variable. Errors on no delay trials (NoDel) were included in the model to control for variance in test performance unrelated to memory. For the foraging task, mean within session errors across all sessions, and acquisition rate (the slope of the logged power curve of latency to reward across subsequent test sessions) were used as dependent variables. Reported F and R^2 values are for the complete regression models. T values and standard error for individual covariates are listed under Factor and SE respectively for each analysis. Results passing significance testing are in bold. '.' $p < 0.10$, '*' $p < 0.05$, '**' $p < 0.01$.

Behavioral Comparison	**Factor**	**SE**	**t**	**F**	**R^2**
Alternation				**5.10****	**0.37**
7s delay vs Rhp & Lhp	**NoDel**	**0.29**	**3.10****		
	Rhp	**25.86**	**-2.82****		
	Lhp	29.39	0.54		
Alternation				**5.76****	**0.40**
7s delay vs vRhp & dRhp	**NoDel**	**0.29**	**3.07****		
	vRhp	79.93	0.24		
	dRhp	**85.00**	**-2.05***		
Foraging Task				**3.54***	**0.24**
In session errors vs	**Rhp**	**5.58**	**-2.66****		
Rhp &Lhp	Lhp	6.61	0.50		
Foraging Task				**4.11***	**0.26**
In session errors vs	vRhp	20.17	0.33		
vRhp & dRhp	**dRhp**	**20.50**	**-1.72.**		
Foraging Task				1.51	0.12
Cross-session acquisition vs	Rhp	1.32	-1.67		
Rhp &Lhp	Lhp	1.57	-0.07		
Foraging Task				**3.78****	**0.42**
Cross-session acquisition vs	**vRhp**	**4.27**	**2.44***		
vRhp, dRhp, vLhp & dLhp	**dRhp**	**4.37**	**-3.21****		
	vLhp	5.05	0.72		
	dLhp	5.61	-1.06		

Table S5 (separate file)

Alternation Task Performance: Latency (in ms) from bucket touchdown to finding the reward location and number of revisits to empty buckets are listed for each daily test session for each subject.

Movie S1

An Example of Free Alternation in the Two-Choice Maze: This video shows one of the study subjects (ID: 8181) navigating the two-choice maze (Fig. S2) during free alternation. A correct choice of door at the end of the maze is rewarded with fish, dispensed from behind the blind seen above on deck.

Movie S2

An Example of Delayed Alternation in the Two-Choice Maze: This video shows one of the study subjects (ID: 8181) navigating the two-choice maze (Fig. S2) with a 7-second delay enforced at the beginning of reach trial. The gate blocking access to the end of the maze is controlled by the experimenter from behind the blind seen above on the deck.

Movie S3

An Example of the Once-Daily Foraging Task: This video shows one of the study subjects (ID: 9821) taking part in a trial on the once-daily foraging task. The buckets are lowered after the subject is baited back to the pool with fish. One of the buckets has fish, and all buckets are removed once the subject has found and eaten the fish and visited all buckets. The fish in this trial are in the left-most bucket from the perspective of the viewer (number 4, Fig. S3).

Archived Database (available at: http://dx.doi.org/10.5061/dryad.0279k)

Functional and Structural Brain Scans: Raw structural and functional brain scans in nifti format for all subjects, as well as the high-resolution (1mm isotropic) structural scan and right and left rostrodorsal thalamic masks used in functional connectivity analysis.

REFERENCES AND NOTES

1. C. A. Scholin, F. Gulland, G. J. Doucette, S. Benson, M. Busman, F. P. Chavez, J. Cordaro, R. DeLong, A. De Vogelaere, J. Harvey, M. Haulena, K. Lefebvre, T. Lipscomb, S. Loscutoff, L. J. Lowenstine, R. Marin 3rd, P. E. Miller, W. A. McLellan, P. D. Moeller, C. L. Powell, T. Rowles, P. Silvagni, M. Silver, T. Spraker, V. Trainer, F. M. Van Dolah, Mortality of sea lions along the central California coast linked to a toxic diatom bloom. *Nature* **403**, 80–84 (2000). Medline doi:10.1038/47481

2. M. W. Silver, S. Bargu, S. L. Coale, C. R. Benitez-Nelson, A. C. Garcia, K. J. Roberts, E. Sekula-Wood, K. W. Bruland, K. H. Coale, Toxic diatoms and domoic acid in natural and iron enriched waters of the oceanic Pacific. *Proc. Natl. Acad. Sci. U.S.A.* **107**, 20762–20767 (2010). Medline doi:10.1073/pnas.1006968107

3. T. Goldstein, J. A. Mazet, T. S. Zabka, G. Langlois, K. M. Colegrove, M. Silver, S. Bargu, F. Van Dolah, T. Leighfield, P. A. Conrad, J. Barakos, D. C. Williams, S. Dennison, M. Haulena, F. M. Gulland, Novel symptomatology and changing epidemiology of domoic acid toxicosis in California sea lions (*Zalophus californianus*): An increasing risk to marine mammal health. *Proc. Biol. Sci.* **275**, 267–276 (2008). Medline doi:10.1098/rspb.2007.1221

4. P. A. Silvagni, L. J. Lowenstine, T. Spraker, T. P. Lipscomb, F. M. D. Gulland, Pathology of domoic acid toxicity in California sea lions (*Zalophus californianus*). *Vet. Pathol.* **42**, 184–191 (2005). Medline doi:10.1354/vp.42-2-184

5. J. O'Keefe, "Nobel lecture: Spatial cells in the hippocampal formation" (Nobel Media AB, 2014); www.nobelprize.org/nobel_prizes/medicine/laureates/2014/okeefe-lecture.html.

6. N. J. Fortin, K. L. Agster, H. B. Eichenbaum, Critical role of the hippocampus in memory for sequences of events. *Nat. Neurosci.* **5**, 458–462 (2002). Medline

7. M. J. Weise, D. P. Costa, R. M. Kudela, Movement and diving behavior of male California sea lions (*Zalophus californianus*) during anomalous oceanographic conditions of 2005 compared to those of 2004. *Geophys. Res. Lett.* **33**, L22S10 (2006). doi:10.1029/2006GL027113

8. K. Thomas, J. T. Harvey, T. Goldstein, J. Barakos, F. M. D. Gulland, Movement, dive behavior, and survival of California sea lions (*Zalophus californianus*) posttreatment for domoic acid toxicosis. *Mar. Mamm. Sci.* **26**, 36–52 (2010). doi:10.1111/j.1748-7692.2009.00314.x

9. Materials and methods are available as supplementary materials on *Science* Online.

10. V. D. Bohbot, M. Kalina, K. Stepankova, N. Spackova, M. Petrides, L. Nadel, Spatial memory deficits in patients with lesions to the right hippocampus and to the right parahippocampal cortex. *Neuropsychologia* **36**, 1217–1238 (1998). Medline doi:10.1016/S0028-3932(97)00161-9

11. M. B. Moser, E. I. Moser, Functional differentiation in the hippocampus. *Hippocampus* **8**, 608–619 (1998). Medline doi:10.1002/(SICI)1098-1063(1998)8:6<608::AID-HIPO3>3.0.CO;2-7

12. W. W. Roberts, W. N. Dember, M. Brodwick, Alternation and exploration in rats with hippocampal lesions. *J. Comp. Physiol. Psychol.* **55**, 695–700 (1962). Medline doi:10.1037/h0045168

13. S. B. Floresco, J. K. Seamans, A. G. Phillips, Selective roles for hippocampal, prefrontal cortical, and ventral striatal circuits in radial-arm maze tasks with or without a delay. *J. Neurosci.* **17**, 1880–1890 (1997). Medline

14. H. Eichenbaum, A cortical-hippocampal system for declarative memory. *Nat. Rev. Neurosci.* **1**, 41–50 (2000). Medline doi:10.1038/35036213

15. D. S. Olton, J. A. Walker, F. H. Gage, Hippocampal connections and spatial discrimination. *Brain Res.* **139**, 295–308 (1978). Medline doi:10.1016/0006-8993(78)90930-7

16. J. M. Parent, T. W. Yu, R. T. Leibowitz, D. H. Geschwind, R. S. Sloviter, D. H. Lowenstein, Dentate granule cell neurogenesis is increased by seizures and contributes to aberrant network reorganization in the adult rat hippocampus. *J. Neurosci.* **17**, 3727–3738 (1997). Medline

17. B. Biswal, F. Z. Yetkin, V. M. Haughton, J. S. Hyde, Functional connectivity in the motor cortex of resting human brain using echo-planar MRI. *Magn. Reson. Med.* **34**, 537–541 (1995). Medline doi:10.1002/mrm.1910340409

18. O. I. Lyamin, I. S. Chetyrbok, Unilateral EEG activation during sleep in the Cape fur seal, Arctocephalus pusillus. *Neurosci. Lett.* **143**, 263–266 (1992). Medline doi:10.1016/0304-3940(92)90279-G

19. S. C. Doney, M. Ruckelshaus, J. E. Duffy, J. P. Barry, F. Chan, C. A. English, H. M. Galindo, J. M. Grebmeier, A. B. Hollowed, N. Knowlton, J. Polovina, N. N. Rabalais, W. J. Sydeman, L. D. Talley, Climate change impacts on marine ecosystems. *Ann. Rev. Mar. Sci.* **4**, 11–37 (2012). Medline doi:10.1146/annurev-marine-041911-111611

20. D. J. Greig, F. M. Gulland, C. Kreuder, A decade of live California sea lion (*Zalophus californianus*) strandings along the central California coast: Causes and trends, 1991–2000. *Aquat. Mamm.* **31**, 11–22 (2005). doi:10.1578/AM.31.1.2005.11

21. E. W. Montie, N. Pussini, G. E. Schneider, T. W. Battey, S. Dennison, J. Barakos, F. Gulland, Neuroanatomy and volumes of brain structures of a live California sea lion (*Zalophus californianus*) from magnetic resonance images. *Anat. Rec.* **292**, 1523–1547 (2009). Medline doi:10.1002/ar.20937

22. M. Jenkinson, C. F. Beckmann, T. E. Behrens, M. W. Woolrich, S. M. Smith, FSL. *Neuroimage* **62**, 782–790 (2012). Medline doi:10.1016/j.neuroimage.2011.09.015

23. K. Niimi, M. Niimi, Y. Okada, Thalamic afferents to the limbic cortex in the cat studied with the method of retrograde axonal transport of horseradish peroxidase. *Brain Res.* **145**, 225–238 (1978). Medline doi:10.1016/0006-8993(78)90859-4